BIAS-CORRECTION IN THE CCAFS-CLIMATE PORTAL: A DESCRIPTION OF MEHOTODOLOGIES

Navarro-Racines, C.E., Tarapues-Montenegro, J.E. and Ramírez-Villegas, J.A.
International Centre for Tropical Agriculture (CIAT). 2015. Contact: c.e.navarro@cgiar.org

How to cite this document?

Navarro-Racines, C.E., Tarapues-Montenegro, J.E and Ramírez-Villegas, J.A. 2015. Bias-correction in the CCAFS-Climate Portal: A description of methodologies. Decision and Policy Analysis (DAPA) Research Area. International Center for Tropical Agriculture (CIAT). Cali, Colombia.

Introduction

Global Climate Models (GCMs) have been the primary source of information for constructing climate scenarios, and they provide the basis for climate change impacts assessments of climate change at all scales, from local to global. However, impact studies rarely use GCM outputs directly because errors in GCM simulations relative to historical observations are large (Ramirez-Villegas et al. 2013), and because the spatial resolution is generally too coarse to satisfy the requirements for finer-scale impact studies. More specifically, the typical GCM spatial resolution (50 km or even more) is not practical for assessing agricultural landscapes, particularly in the tropics, where orographic and climatic conditions vary significantly across relatively small distances (Tabor & Williams, 2010). Hence, it is important to bias-correct and downscale the raw climate model outputs in order to produce climate projections that are better fit for agricultural modeling. Here we describe three different calibration approaches to produce reliable daily climate for future periods, employed in a new interface in CCAFS-Climate portal (http://www.ccafs-climate.org/data_bias_correction/), as follows: (a) bias correction (or nudging) (Hawkins et al., 2013), (b) change factor (Hawkins et al., 2013) and (c) Quantile Mapping (Gudmundsson et al., 2012). In addition, briefly describe some observational datasets relevant to agricultural modeling and employed as the historical observations for the calibration methods mentioned here.

Observational Datasets

The methods described below must be applied to the historical observations to produce calibrated projections of future climate. Thus, we selected six widely used datasets that could be used to "calibrate" daily outputs of GCMs from the IPCC CMIP5. All datasets are bias-corrected versions of existing reanalysis datasets. A reanalysis involves reprocessing observational data spanning an extended historical period using a consistent analysis system, to produce a dataset that can be used for meteorological and climatological studies. In the Table 1 are described some characteristics of these datasets.

Table 1. Observational datasets features

Dataset	Based on	Period	Resolution	Main Reference
AgCFSR	The Modern-Era Retrospective Analysis for Research and Applications (MERRA).	1980–2010	0.25° × 0.25°	Ruane et al. (2015)
AgMerra	The Climate Forecast System Reanalysis (CFSR)	1980–2010	0.25° × 0.25°	Ruane et al. (2015)
GRASP	ERA-40 JRA-25	1961–2010	1.125° × 1.125°	Iizumi et al. (2014)
Princeton	Reanalysis-1	1948–2008	0.5° × 0.5°	Sheffield et al. (2006)
WFD	ERA-40	1958–2001	0.5° × 0.5°	Weedon et al. (2011)
WFDEI	ERA-Interim	1979–2009	0.5° × 0.5°	Weedon et al. (2011)

Bias Correction

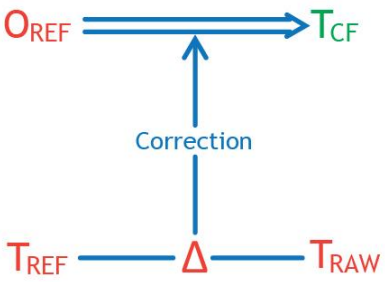

The Bias Correction (BC) approach corrects the projected raw daily GCM output using the differences in the mean and variability between GCM and observations in a reference period (Figure 1).

Figure 1. Schematic of the bias correction methodology. BC uses raw model output for the future period, and corrects it using the differences (Δ) between historical reference data from the model and observations. (O_{REF} = observations in the historical reference period; T_{REF} = GCM output from the historical reference period; T_{RAW} = raw GCM output for the historical or future period; T_{BC} = bias-corrected GCM output.)

If we assumed the variability as equal both for GCMs and observations, the daily data is simply shifted by the mean bias in the reference period (Hawkins et al., 2013), thus:

$$T_{BC}(t) = T_{RAW}(t) - \overline{T_{REF}} \qquad \textbf{Eq. 1}$$

However, it is possible to apply a more general form of this bias-correction method that corrects not only the mean values but also the temporal variability of the model output in accordance with the observations (Hawkins et al., 2013; Ho et al., 2012):

$$T_{BC}(t) = \overline{O_{REF}} + \frac{\sigma_{O,REF}}{\sigma_{T,REF}}(T_{RAW}(t) - \overline{T_{REF}}) \qquad \textbf{Eq. 2}$$

where $\sigma_{T,REF}$ and $\sigma_{O,REF}$ represent the standard deviation in the reference period of the daily GCM output and observations, respectively. Note that this bias-correction procedure for the GCM output could be applied to correct both the historical and future periods.

Change Factor

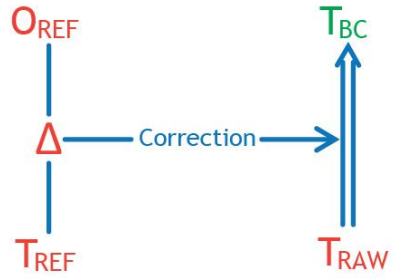

In the Change Factor (CF) approach the raw GCM outputs current values are subtracted from the future simulated values, resulting in "climate anomalies" which are then added to the present day observational dataset (Tabor & Williams, 2010).

Figure 2. Schematic of the change factor methodology. CF uses present day observations, corrected using the differences (Δ) between present and future model data. (O_{REF} = observations in the historical reference period; T_{REF} = GCM output from the historical reference period; T_{RAW} = raw GCM output for the historical or future period; T_{BC} = change factor-corrected GCM output.)

When the daily variability is assumed of the same magnitude in the future and reference periods, the method is called 'delta method', and the corrected daily data is:

$$T_{CF}(t) = O_{REF}(t) + (\overline{T_{RAW}} - \overline{T_{REF}}) \qquad \textbf{Eq. 3}$$

But, the more general form considering changes in variance (Ho et al., 2012), is:

$$T_{CF}(t) = \overline{T_{RAW}} + \frac{\sigma_{T,RAW}}{\sigma_{T,REF}}(O_{REF}(t) - \overline{T_{REF}}) \qquad \textbf{Eq. 4}$$

where $\sigma_{T,RAW}$ and $\sigma_{O,REF}$ represent the standard deviation in the future period of the daily GCM output and observations, respectively.

Quantile Mapping

The above-described methods work well for more non-stochastic variables (i.e. temperature). A more sophisticated approach for bias-correcting more stochastic variables (e.g. precipitation and solar radiation) is needed. This is because for example, GCM outputs are known to have a "drizzle problem," that is, too many low-magnitude rain events as compared to observations (Gutowski et al., 2003). Also, GCMs do not capture realistic interannual variability associated with events such as El Niño and La Niña.

In order to appropriately bias-correct GCM output for monthly totals and wet-day frequency, while ensuring realistic daily and interannual variability, we implemented the Quantile Mapping (QM) approach with the qmap library written for R statistical software (Gudmundsson, 2014; Gudmundsson et al., 2012). The quantile mapping technique removes the systematic bias in the GCM simulations and has the benefit of accounting for GCM biases in all statistical moments, though, like all statistical downscaling approaches, it is assumed that biases relative to historical observations will be constant in the projection period (Thrasher et al., 2012).

Annex. A quick comparison

Here, we show a site-specific comparison between raw GCM output, bias-corrected climate variables with the methodologies described, and historical observations, for one GCM (BNU-ESM) and for three different metrics:

- Daily time series (Figure 3-6) for present day conditions (1980–2005) and future (2040-2065).
- Rainfall frequency (Figure 7) and hot day frequency (days with more than 30°C, Figure 8) , with monthly values averaged across 1980–2005 and 2040-2065.
- Interannual variability expresed as standard deviation of monthly precipitation (Figure 9) and mean maximum temperature values (Figure 10) for present day (1980–2005) and future (2040-2065) conditions.
- Density plot (Figures 11-12)..
- Projected change (Figure 13).

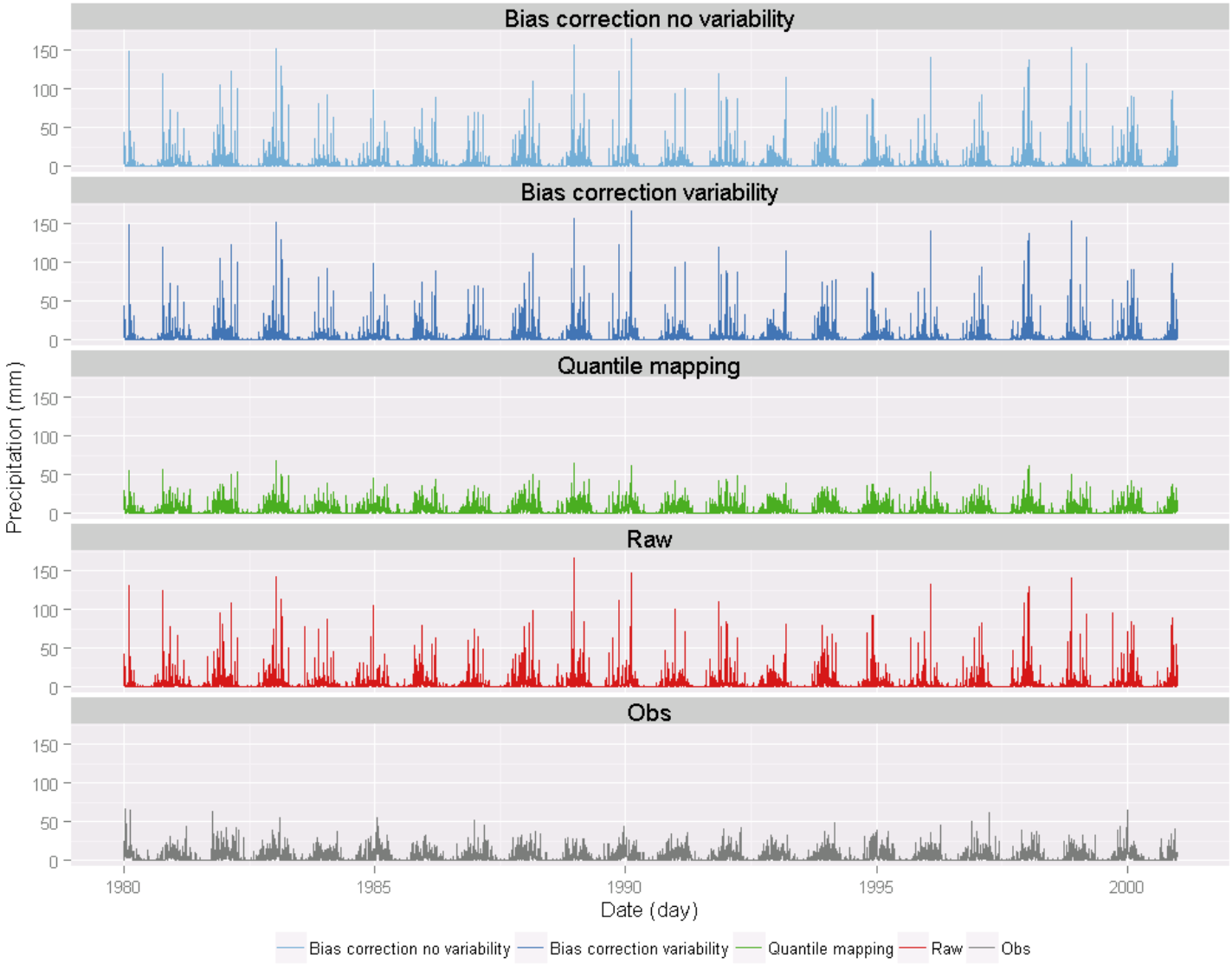

Figure 3. Comparison of daily precipitation for present day conditions 1980-2005 between raw GCM model output (red), the historical observations (gray) and the bias-corrected GCM model output for BC (blue) and QM (green) approaches. Blue lighter lines include variability for BC.

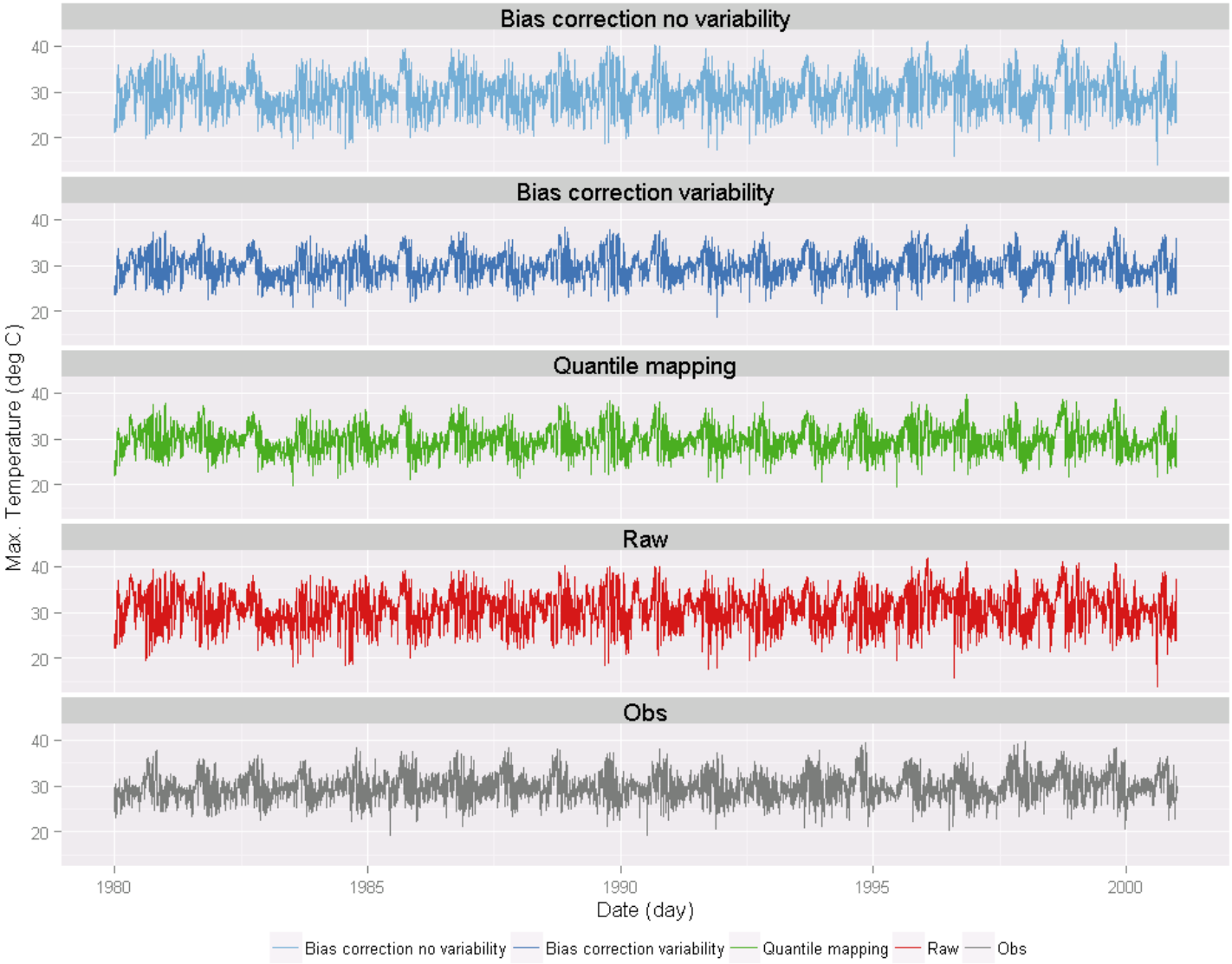

Figure 4. Comparison of daily maximum temperature for present day conditions 1980-2005 between raw GCM model output (red), the historical observations (gray) and the bias-corrected GCM model output for BC (blue) and QM (green) approaches. Blue lighter line include variability for BC.

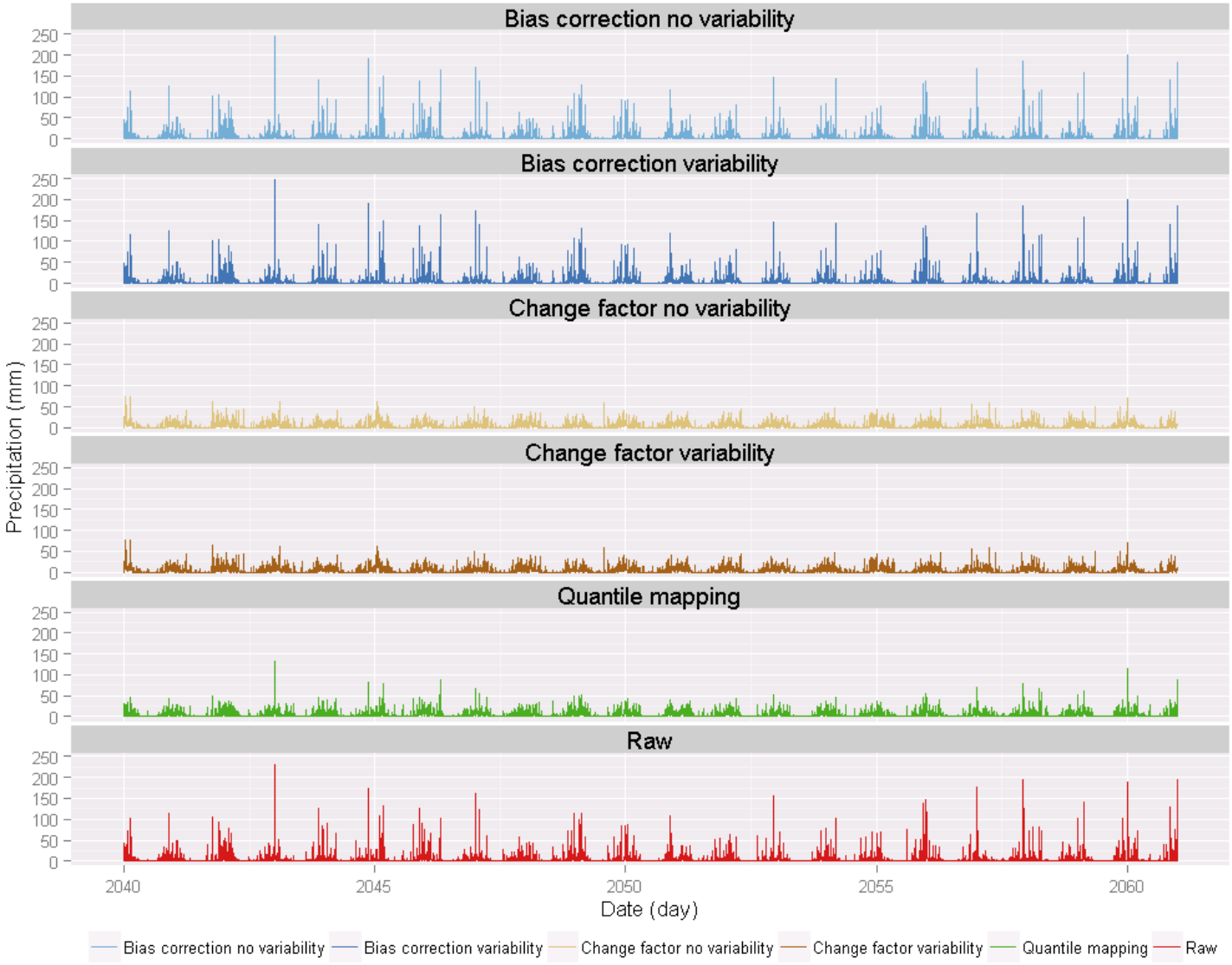

Figure 5. Comparison of daily precipitation for future 2040-2065 between raw GCM model output (red) and the bias-corrected GCM model output for BC (blue), CF (brown) and QM (green) approaches. Blue and brown lighter lines include variability for BC and CF respectively.

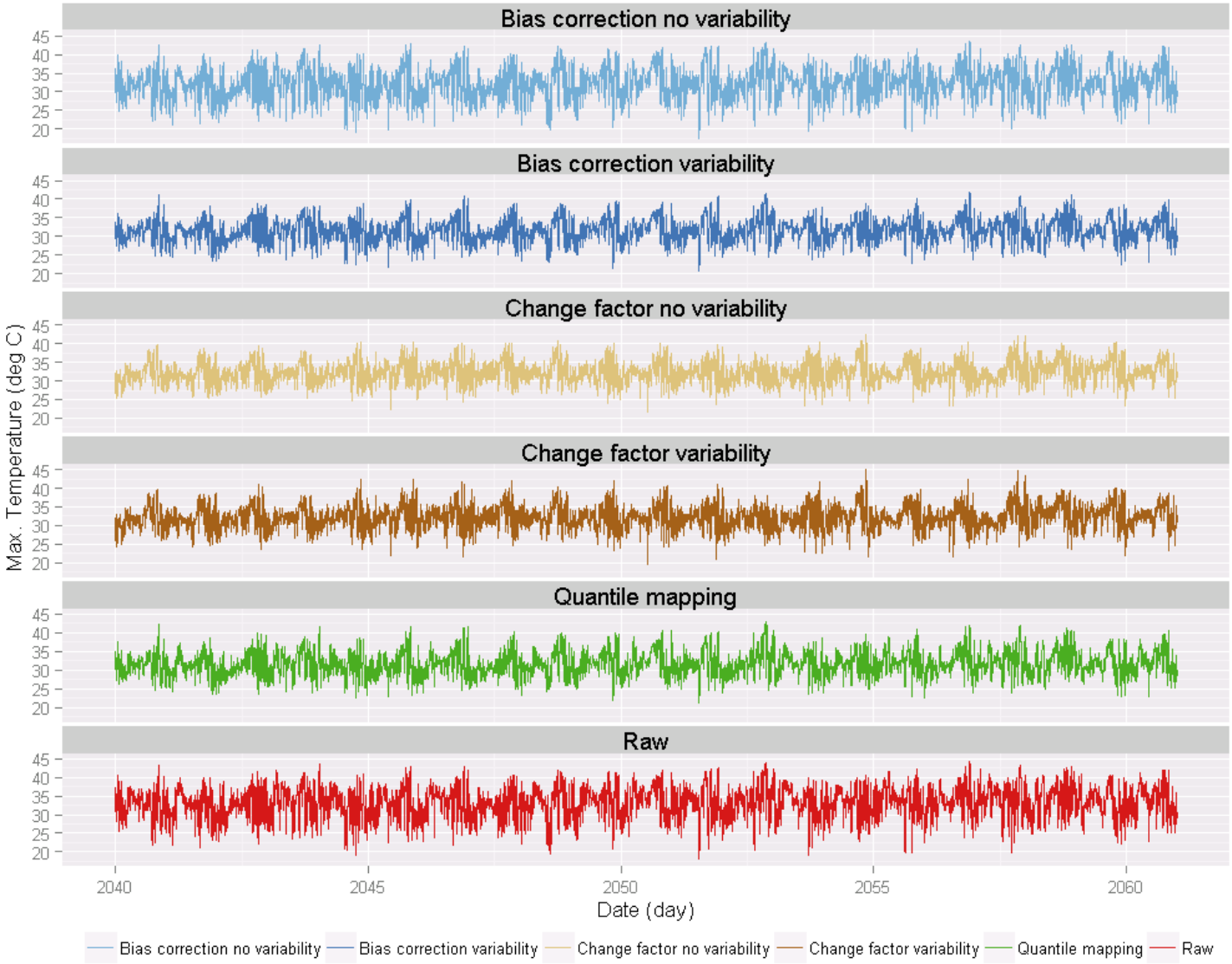

Figure 6. Comparison of daily maximum temperature for future 2040-2065 between raw GCM model output (red) and the bias-corrected GCM model output for BC (blue), CF (brown) and QM (green) approaches. Blue and brown lighter lines include variability for BC and CF respectively.

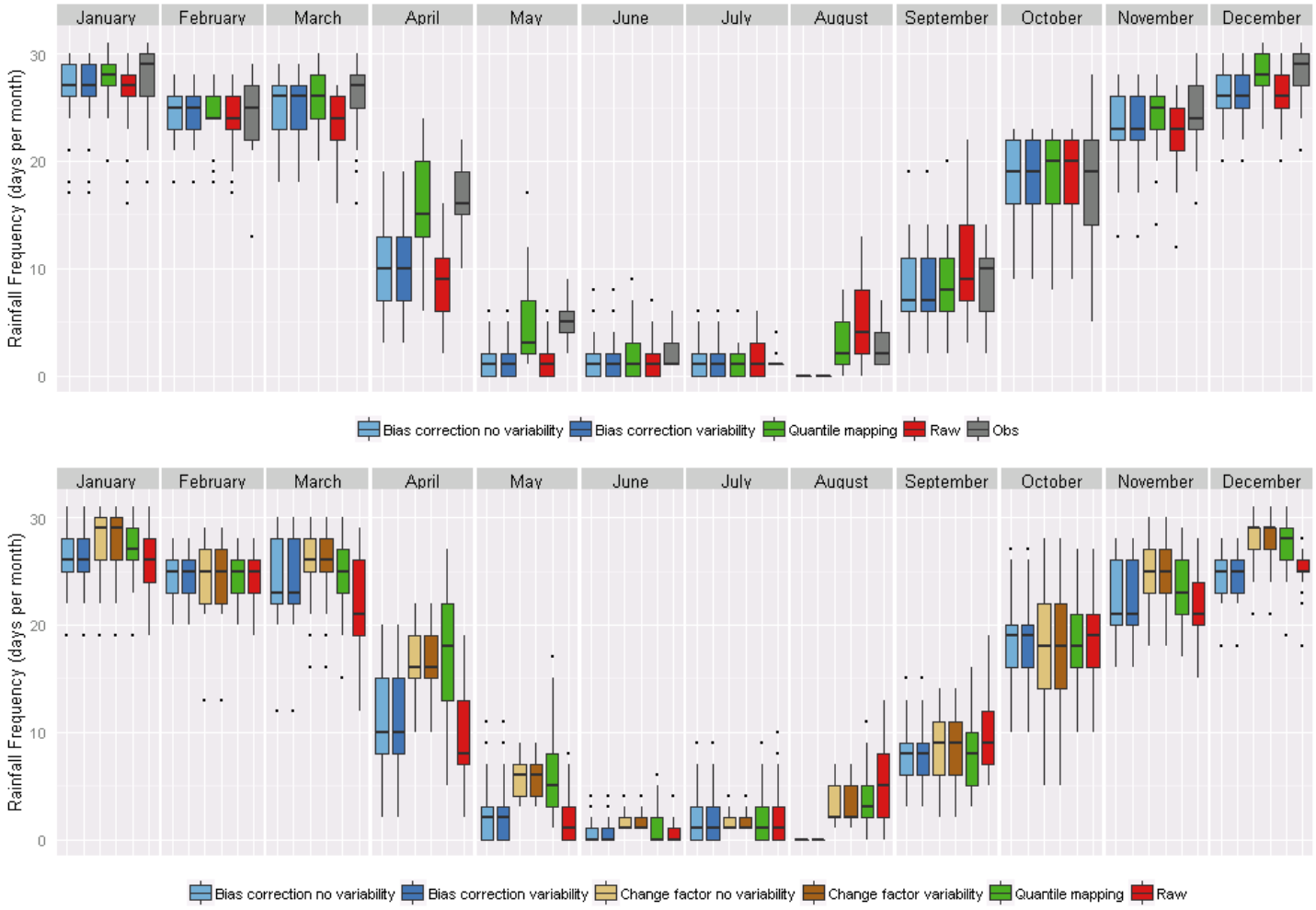

Figure 7. Rainfall frequency (in days/month where a rainy day is defined as having ≥1 mm precipitation) for raw GCM model output (red), the historical observations (gray) and the bias-corrected GCM model output for BC (blue), CF (brown) and QM (green) approaches. Blue and brown lighter boxplot include variability for BC and CF respectively. Monthly box plots represent the median and spread for each month across years from 1980-2005 (top) and 2040-2065 (bottom).

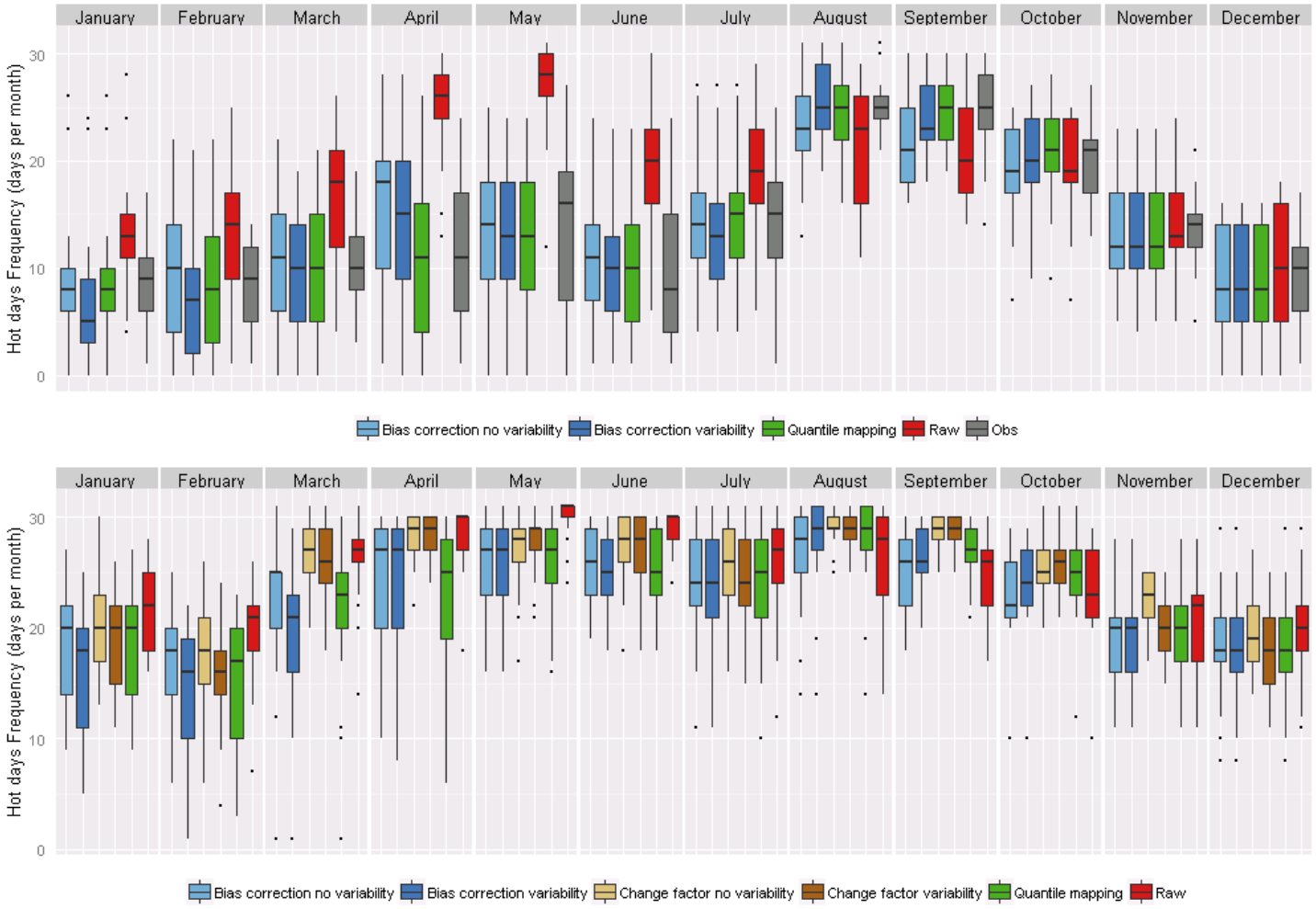

Figure 8. Frequency of hot days (in days/month where a hot day is defined as having ≥30 °C maximum temperature) for raw GCM model output (red), the historical observations (gray) and the bias-corrected GCM model output for BC (blue), CF (brown) and QM (green) approaches. Blue and brown lighter boxplot include variability for BC and CF respectively. Monthly box plots represent the median and spread for each month across years from 1980-2005 (top) and 2040-2065 (bottom).

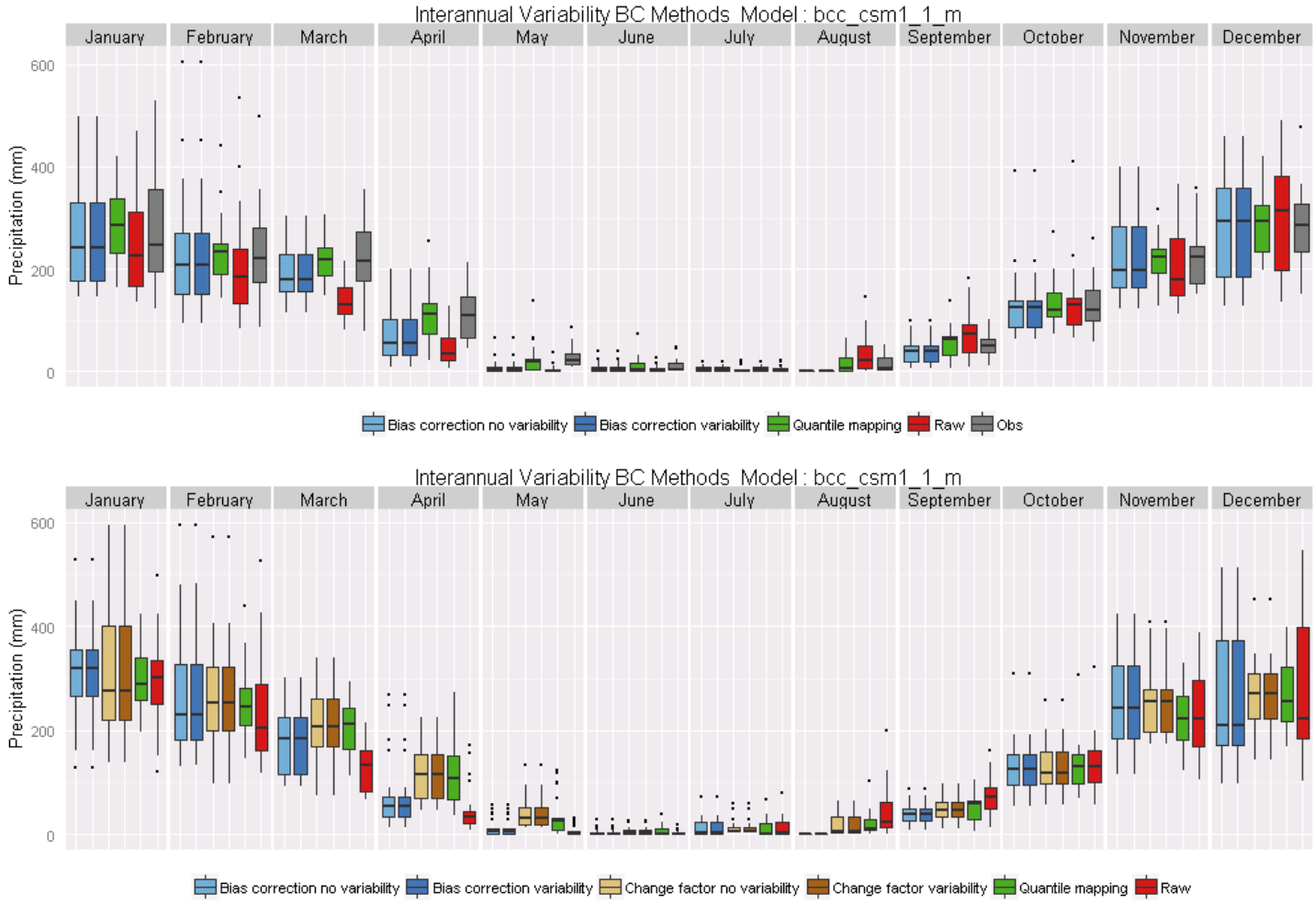

Figure 9. Interannual variability of monthly precipitation, for raw GCM model output (red), the present day observations (gray) and the bias-corrected GCM model output for BC (blue), CF (brown) and QM (green) approaches. Blue and brown lighter boxplot include variability for BC and CF respectively.

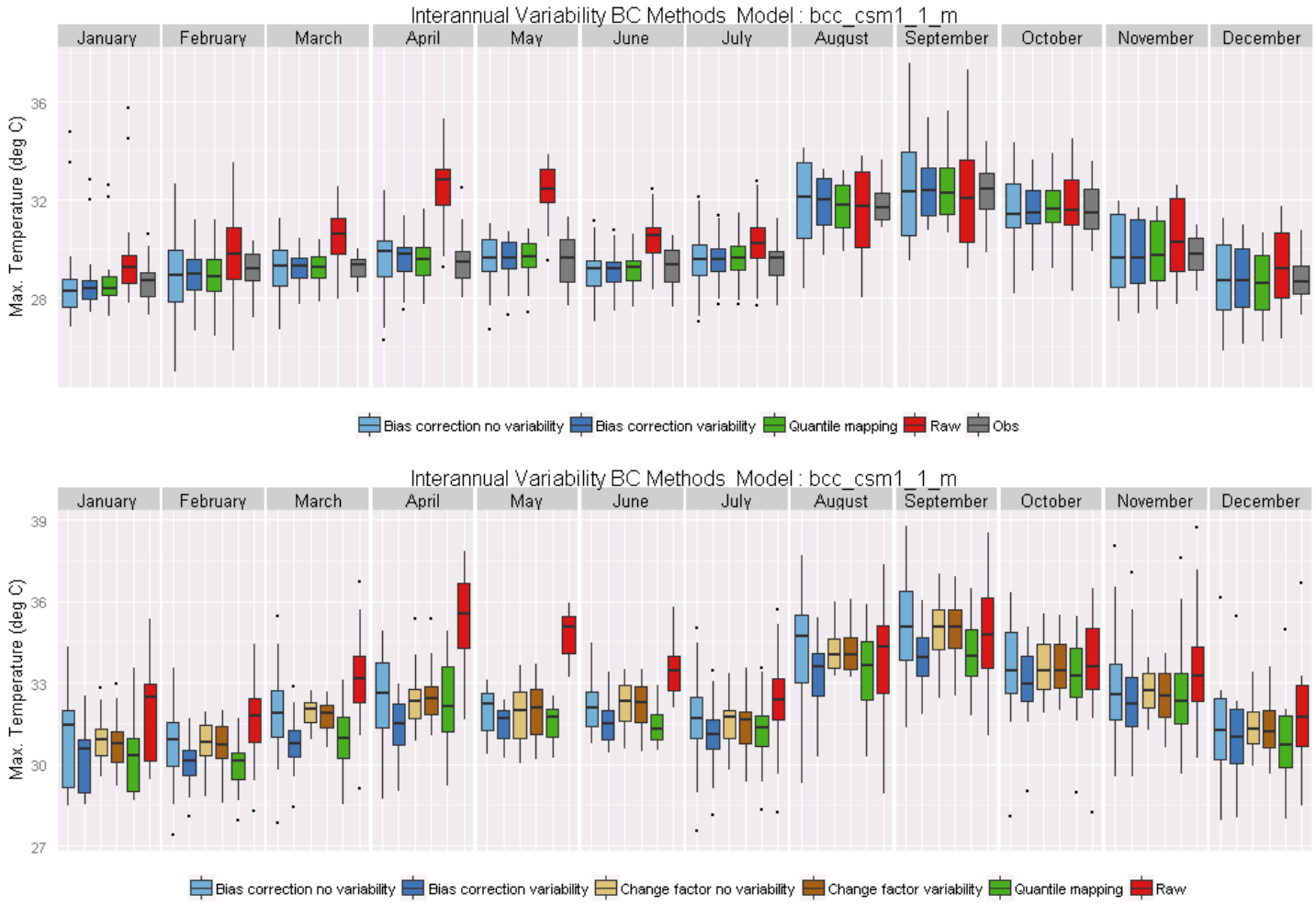

Figure 10. Interannual variability of mean monthly maximum temperature for raw GCM model output (red) and the bias-corrected GCM model output for BC (blue), CF (brown) and QM (green) approaches. Blue and brown lighter boxplot include variability for BC and CF respectively.

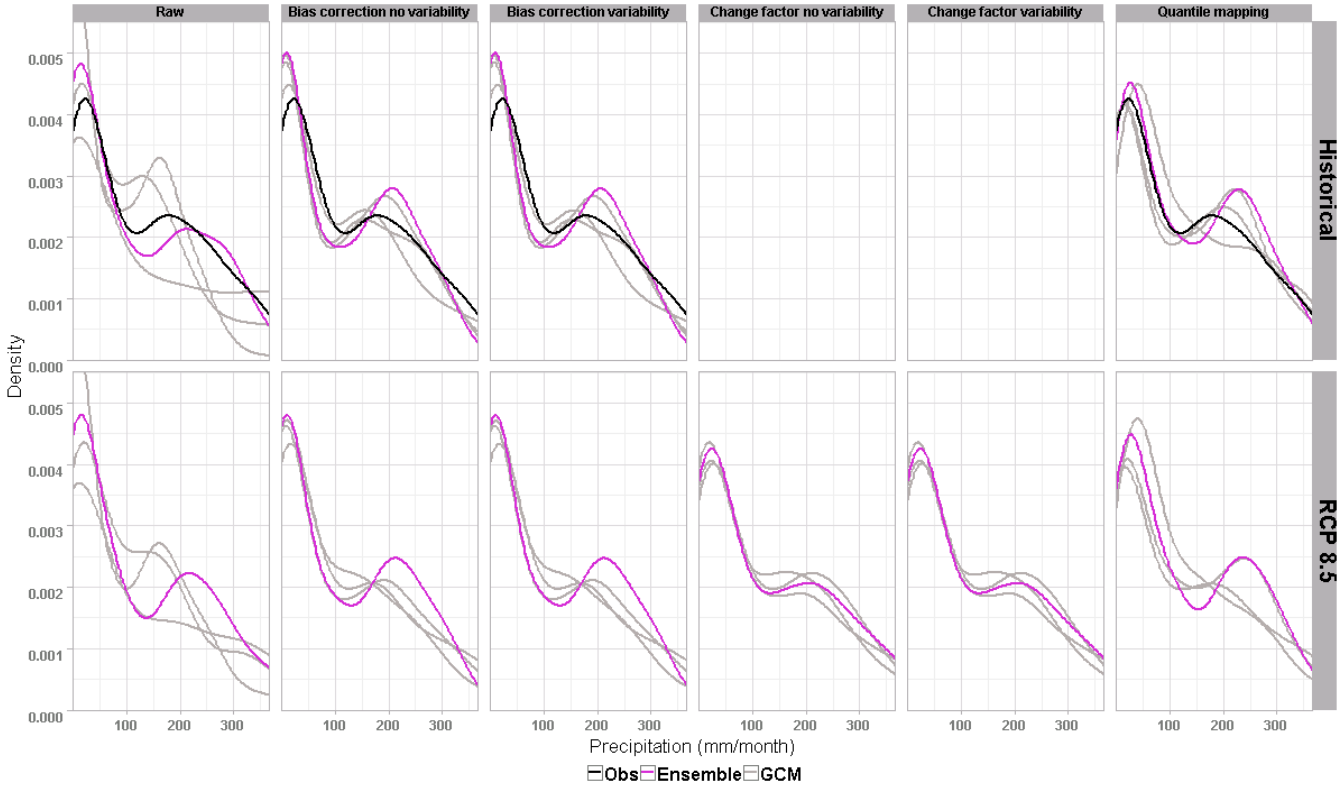

Figure 11. Comparison of monthly precipitation density (pixel density) for present day conditions 1980-2005 and future 2040-2065 between 5 methods of bias Correction. GCM model ensemble (purple), GCM individual models (gray) and the historical observations (black).

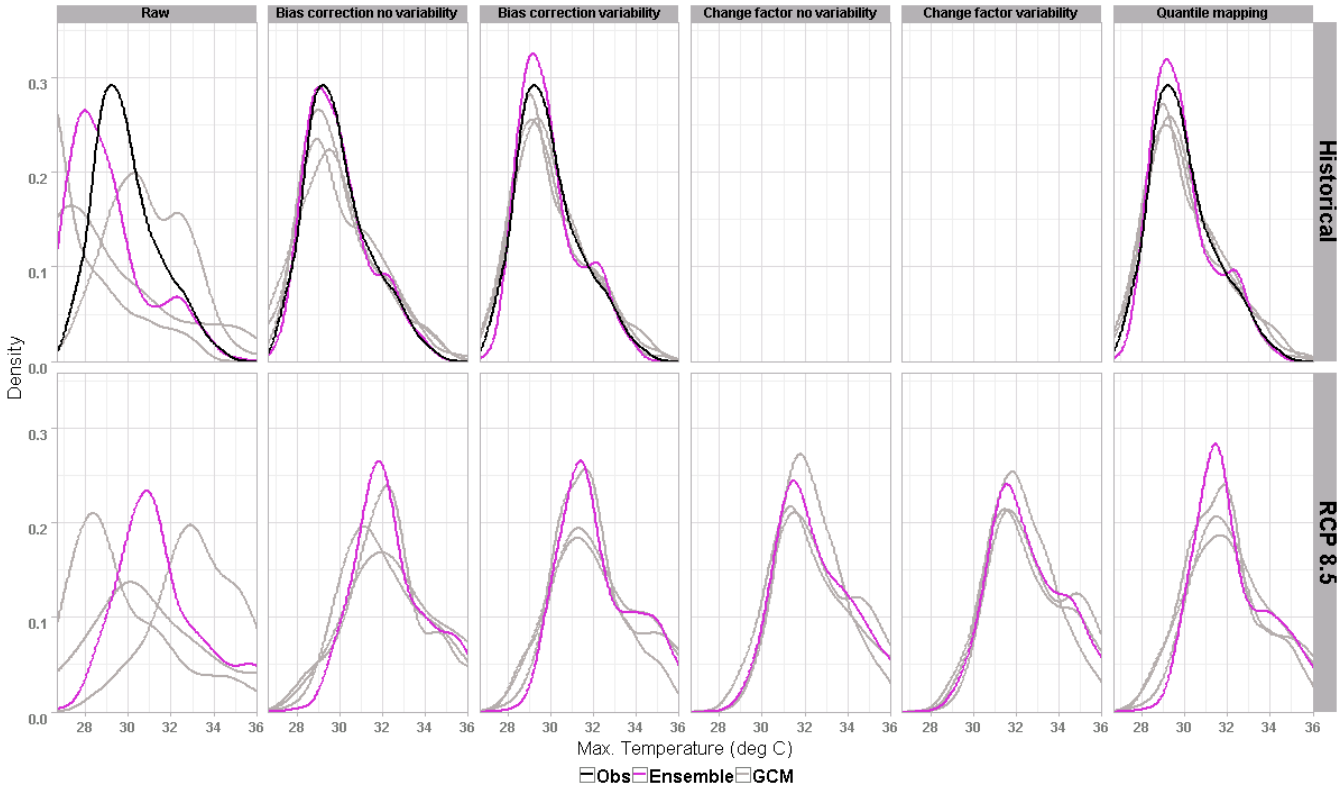

Figure 12. Comparison of monthly mean maximum temperature density (pixel density) for present day conditions 1980-2005 and future 2040-2065 between 5 methods of bias Correction. GCM model ensemble (purple), GCM individual models (gray) and the historical observations (black).

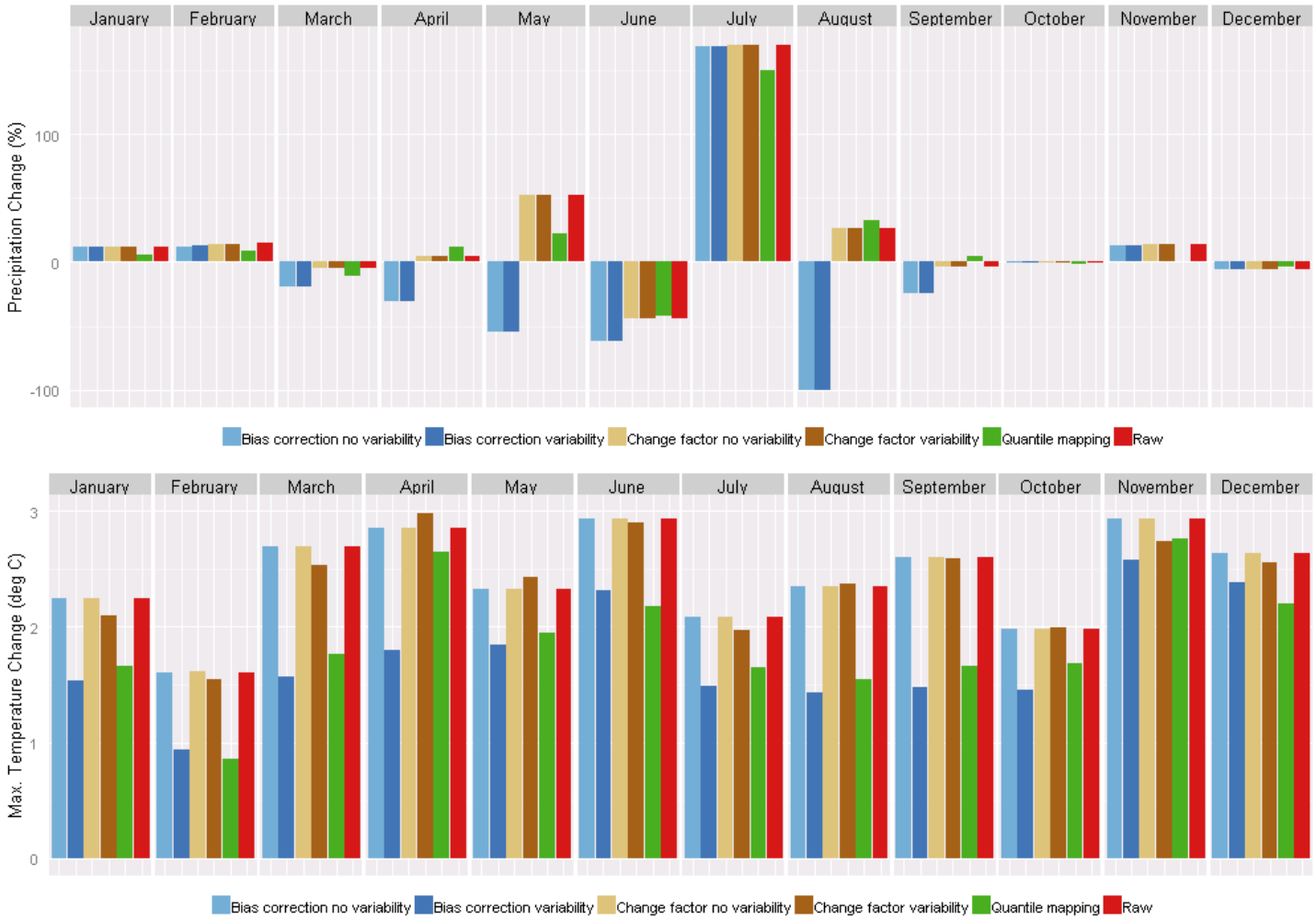

Figure 13. Projected change of monthly precipitation (top) and mean monthly maximum temperature (above) for raw GCM model output (red) and the bias-corrected GCM model output for BC (blue), CF (brown) and QM (green) approaches.

References

Gudmundsson, L. (2014). Qmap: Statistical transformations for post-processing climate model output.

Gudmundsson, L., Bremnes, J. B., Haugen, J. E., & Engen-Skaugen, T. (2012). Technical Note: Downscaling RCM precipitation to the station scale using statistical transformations – a comparison of methods. *Hydrol. Earth Syst. Sci.*, *16*(9), 3383–3390. http://doi.org/10.5194/hess-16-3383-2012

Gutowski, W. J., Decker, S. G., Donavon, R. A., Pan, Z., Arritt, R. W., & Takle, E. S. (2003). Temporal–Spatial Scales of Observed and Simulated Precipitation in Central U.S. Climate. *Journal of Climate*, *16*(22), 3841–3847. http://doi.org/10.1175/1520-0442(2003)016<3841:TSOOAS>2.0.CO;2

Hawkins, E., Osborne, T. M., Ho, C. K., & Challinor, A. J. (2013). Calibration and bias correction of climate projections for crop modelling: An idealised case study over Europe. *Agricultural and Forest Meteorology*, *170*(0), 19–31. http://doi.org/http://dx.doi.org/10.1016/j.agrformet.2012.04.007

Ho, C. K., Stephenson, D. B., Collins, M., Ferro, C. a T., & Brown, S. J. (2012). Calibration strategies; a source of additional uncertainty in climate change projections. *Bulletin of the American Meteorological Society*, *93*(1), 21–26. http://doi.org/10.1175/2011BAMS3110.1

Iizumi, T., Okada, M., & Yokozawza, M. (2014). A meteorological forcing data set for global crop modeling: Development, evaluation, and intercomparison. *Journal of Geophysical Research: Atmospheres*, *119*(2), 363–384. http://doi.org/10.1002/2013JD020130

Ramirez-Villegas, J., Challinor, A.J., Thornton, P.K., & Jarvis, A. (2013). *Implications of regional improvement in global climate models for agricultural impact research. Environ Res Lett* 8:24018.

Ruane, A. C., Cecil, L. D., Horton, R. M., Gordón, R., McCollum, R., Brown, D., Killough, B., Goldberg, R., Greeley, A. P., & Rosenzweig, C. (2011). Climate change impact uncertainties for maize in Panama: Farm information, climate projections, and yield sensitivities. *Agricultural and Forest Meteorology*, (0). http://doi.org/10.1016/j.agrformet.2011.10.015

Ruane, A. C., Goldberg, R., & Chryssanthacopoulos, J. (2015). Climate forcing datasets for agricultural modeling: Merged products for gap-filling and historical climate series estimation. *Agricultural and Forest Meteorology*, *200*, 233–248. http://doi.org/http://dx.doi.org/10.1016/j.agrformet.2014.09.016

Sheffield, J., Goteti, G., & Wood, E. F. (2006). Development of a 50-Year High-Resolution Global Dataset of Meteorological Forcings for Land Surface Modeling. *Journal of Climate*, *19*(13), 3088–3111. http://doi.org/10.1175/JCLI3790.1

Tabor, K., & Williams, J. W. (2010). Globally downscaled climate projections for assessing the conservation impacts of climate change. *Ecological Applications*, *20*(2), 554–565. Retrieved from http://ccr.aos.wisc.edu/publications/pdfs/globaldownscale.pdf

Thrasher, B. L., Maurer, E. P., McKellar, C., & Duffy, P. B. (2012). Technical Note: Bias correcting climate model simulated daily temperature extremes with quantile mapping. *Hydrol. Earth Syst. Sci. Discuss.*, *9*(4), 5515–5529. http://doi.org/10.5194/hessd-9-5515-2012

Weedon, G. P., Gomes, S., Viterbo, P., Shuttleworth, W. J., Blyth, E., Österle, H., Adam, J. C., Bellouin, N., Boucher, O., & Best, M. (2011). Creation of the WATCH Forcing Data and Its Use to Assess Global and Regional Reference Crop Evaporation over Land during the Twentieth Century. *Journal of Hydrometeorology*, *12*(5), 823–848. http://doi.org/10.1175/2011JHM1369.1